

Supplementary Materials

File S1

Details of the algorithm magicMap

HMM

The HMM in multiparental populations has been described in detail for haplotype reconstruction (Zheng *et al.* 2015) and genotype imputation (Zheng *et al.* 2018a). Here we give a short summary. Conditional on phased parental genotypes, offspring are assumed to be independent. The hidden process describes how the ancestral origins change along the two homologous chromosomes within an offspring. It is assumed to follow a continuous time Markov process, which is described by an initial distribution π and a rate matrix Q . The initial distribution π is specified to be the stationary distribution of the rate matrix, so that the prior ancestral origin process does not depend on chromosome direction. According to the theory of continuous time Markov chain, the transition probability matrix from markers t to $t + 1$ is in the form of the matrix exponential

$$P[x_{t+1}|x_t, d_t] = e^{Qd_t},$$

where $x_t = (x_t^m, x_t^p)$ with x_t^m (x_t^p) being the ancestral origin on the maternally (paternally) derived chromosome at marker t , and d_t is the genetic distance in Morgan between markers t and $t + 1$.

The calculation of the rate matrix Q depends the relationship between the two homologous chromosomes within an offspring. Following Zheng *et al.* (2015), "depModel" denotes the ancestral origin process along the maternally derived chromosome is completely determined by the ancestral origin process along the paternally derived chromosome, "indepModel" denotes that the two ancestral origin processes are independent, and "jointModel" denotes that two processes are modeled jointly. Here we assume that there is no genetic interference. The rate matrix Q takes a general form for "jointModel". It holds that $Q = Q^m \otimes I + I \otimes Q^p$ for "indepModel", where Q^m (Q^p) denotes the rate matrix for the continuous time Markov processes along the maternally (paternally) derived chromosome, \otimes denotes the Kronecker product, and I is an identity matrix with appropriate dimension. For "depModel", we only need to consider one representative homologous chromosome, and the rate matrix $Q = (Q^m + Q^p)/2$ for autosomes or female X chromosomes, and $Q = Q^m$ for male X

25 chromosomes. The calculations of π , Q^m , Q^p , and Q using the available breeding design information have
 26 been described (Zheng *et al.* 2014; Zheng 2015; Zheng *et al.* 2018b).

27 For example, consider four-way RILs by many generations of selfing so that the population becomes fully
 28 inbred. We use "depModel" for the ancestral origin process. The rate matrix is given by

$$Q = \begin{pmatrix} -1 & 1/3 & 1/3 & 1/3 \\ 1/3 & -1 & 1/3 & 1/3 \\ 1/3 & 1/3 & -1 & 1/3 \\ 1/3 & 1/3 & 1/3 & -1 \end{pmatrix} R,$$

29 and the transition probability matrix is given by

$$P(x_{t+1}|x_t) = e^{Qd_t} = \begin{pmatrix} 1 - 3r/4 & r/4 & r/4 & r/4 \\ r/4 & 1 - 3r/4 & r/4 & r/4 \\ r/4 & r/4 & 1 - 3r/4 & r/4 \\ r/4 & r/4 & r/4 & 1 - 3r/4 \end{pmatrix}$$

30 where the state space consists of four inbred founder origins, $1/3$ denotes the probability that current state
 31 changes into one of other three equally probable parental origins, the map expansion R denotes the average
 32 number of recombination breakpoints per Morgan and $R = 3$ for four-way RILs by selfing, and the scaled
 33 recombination fraction r is given by

$$r = 1 - e^{-\frac{4}{3}Rd_t},$$

34 which is similar to the Haldane's map function. Here we have scaled the recombination fraction so that the
 35 maximum value is always 1, independent of the number of founders.

36 **Two-locus linkage analysis**

37 We denote the two loci by subscripts 1 and 2. For the sake of computational efficiency in two-locus linkage
 38 analysis but not in the final map refinement stage, we construct the transition probability from the stationary
 39 distribution vector $\pi(x)$ instead of the rate matrix \mathbf{Q} , and allow only "depModel" and "indepModel". For a
 40 maternally or paternally derived homologous chromosome, the transition probability matrix is constructed as
 41 follow,

$$P[x_2^a|x_1^a, r] = (1 - r)\mathbf{I}_n + r[\mathbf{1}_n \otimes \pi(x_2^a)], a = m, p$$

42 where $\mathbf{1}_n$ is a vector with all elements being 1, the first term on the right-hand side denotes the case of
 43 no recombination, and the second term denotes that x_2^a follows the stationary distribution in the case of
 44 recombination. For "depModel", the transition probability matrix $P(x_2|x_1, r)$ is calculated as $\frac{1}{2}P[x_2^m|x_1^m, r] +$
 45 $\frac{1}{2}P[x_2^p|x_1^p, r]$ for autosomes or female X chromosome, and $P[x_2^m|x_1^m, r]$ for male X chromosomes. For
 46 "indepModel", it is given by $P[x_2^m|x_1^m, r] \otimes P[x_2^p|x_1^p, r]$.

47 Offspring are assumed to be independent conditional on parental haplotypes, and thus the likelihood l for all
 48 offspring is given by

$$l(r, h_1, h_2) = \prod_o P(y_1^o, y_2^o|r, h_1, h_2),$$

$$P(y_1^o, y_2^o|r, h_1, h_2) = \sum_{x_1, x_2} P(y_1^o|x_1, h_1, \epsilon, \epsilon_F)P(y_2^o|x_2, h_2, \epsilon, \epsilon_F)P(x_2|x_1, r)\pi(x_1),$$

49 where r is scaled recombination fraction with maximum being 1, parental haplotype h_i ($i = 1, 2$) accounts
 50 for missing genotypes in founders and unknown parental genotype phases, ϵ (ϵ_F) denotes the probability of
 51 allelic errors in offspring (founders), and $P(y_i^o|x_i, h_i, \epsilon, \epsilon_F)$ ($i = 1, 2$) is the probability of genotype y_i^o of
 52 offspring o and it is described in [Zheng et al. \(2015, 2018a\)](#). Since the transition probability matrix element
 53 $P(x_2|x_1, r)$ is a polynomial function of r , the individual likelihood $P(y_1^o, y_2^o|r, h_1, h_2)$ can also be expressed as
 54 a polynomial function of r . The function is linear for "depModel" and quadratic for "indepModel". Because
 55 both genotypes y_i^o and parental haplotypes h_i ($i = 1, 2$) take only discrete values, we calculate individual
 56 likelihood $P(y_1^o, y_2^o|r, h_1, h_2)$ as a polynomial function of r for all possible combinations of genotypes and

57 haplotypes, which can be saved in a table to increase computational efficiency. For each pair of markers, we
 58 estimate scaled recombination fraction r and parental haplotypes h_1 and h_2 by maximizing the likelihood
 59 $l(r, h_1, h_2)$ using Brent's numerical method (Brent 1973), and calculate the linkage LOD score under the null
 60 model of $r = 1$.

61 **Spectral clustering**

62 Given the weight matrix W , we group markers based on the spectral clustering algorithm (Shi and Malik 2000)
 63 that uses a tool called graph Laplacian. The three variants of graph Laplacians are given by

$$L = D - W,$$

$$L_{sym} = I - D^{-1/2}WD^{-1/2},$$

$$L_{rw} = I - D^{-1}W$$

64 where D is the degree matrix, a diagonal matrix with i th diagonal element being $\sum_j w_{ij}$. All three graph
 65 Laplacians are positive semi-definite and have non-negative and real-valued eigenvalues. The number of
 66 connected components of the similarity graph is given by the number of zero eigenvalues, and the components
 67 can be specified according to the corresponding eigenvectors. The random walk related L_{rw} is more favored
 68 than the symmetric normalized L_{sym} and the unnormalized L (von Luxburg 2007), and thus it is used by default
 69 in our method.

70 In relation to the variants of graph Laplacians, there are also several well-known versions of spectral
 71 clustering algorithms. We describe as follows a modified version of spectral clustering for marker grouping
 72 with the input being the weight matrix W and the number n_{group} of groups to construct.

- 73 1. Compute the graph Laplacian L_{rw} from the weight matrix W .
- 74 2. Compute the first $2n_{group}$ eigenvalues and eigenvectors of L_{rw} , which are ordered with increasing
 75 eigenvalues.
- 76 3. Select the first $n_{group} \leq n' \leq 2n_{group}$ eigenvectors so that the ratio of the $(n' + 1)^{th}$ to the $(n')^{th}$
 77 eigenvalues is a local maximum.
- 78 4. Let U be the matrix using the n' eigenvectors as columns.
- 79 5. Cluster the rows of U with the agglomerative hierarchical clustering algorithm with linkage being average

80 and distance metric being cosine.

81 where in the last step the simple k -means algorithm with the Euclidean distance that is used in the spectral
82 clustering (Shi and Malik 2000) is replaced by the hierarchical clustering with the cosine distance, because the
83 latter has been observed with better performance in our preliminary simulation studies. In addition, we select
84 eigenvectors in steps 2 and 3, in contrast to the usual spectral clustering algorithm that uses only the first n_{group}
85 eigenvectors; the maximum number $2n_{group}$ of eigenvectors for selection is somewhat arbitrary.

86 **Spectral ordering**

87 In comparison with spectral clustering, spectral ordering uses a single eigenvector of graph Laplacian for
88 ordering vertices of a connected similarity graph. Let $\mathbf{q} = (q_1, q_2, \dots, q_n)$ be the relative ordering of n markers
89 in a given linkage group, subject to rescaling and shifting. The goal of spectral ordering is to place similar
90 markers in adjacent orders and to place dissimilar markers far apart. Formally, it minimizes the following
91 weighted sum of squares

$$f(\mathbf{q}) = \frac{1}{2} \sum_{i,j} (q_i - q_j)^2 w_{ij} = \mathbf{q}' \mathbf{L} \mathbf{q},$$

92 subject to the constraints $\mathbf{q}' \mathbf{1} = 0$ and $\mathbf{q}' \mathbf{q} = 1$, where the prime $'$ denotes transpose, and $\mathbf{1} = (1, \dots, 1)$. The
93 solution \mathbf{q} satisfies the eigenvalue equation $\mathbf{L} \mathbf{q} = \lambda \mathbf{q}$ under the second constraint. The trivial eigenvector
94 corresponding to eigenvalue $\lambda = 0$ is $\mathbf{q} = \mathbf{1}$. The markers are ordered by the element values of the Fiedler
95 vector, the eigenvector associated with the non-zero smallest eigenvalue (Fiedler 1973, 1989).

96 Ding and He (2004) described a modified version using the weighted constraints $\mathbf{q}' \mathbf{D} \mathbf{1} = 0$ and $\mathbf{q}' \mathbf{D} \mathbf{q} = 1$,
97 and the Fiedler vector satisfies $\mathbf{L}_{rw} \mathbf{q} = \lambda \mathbf{q}$. The authors have shown that the weighting leads to better ordering
98 because it tends to keep vertices with more edges in the middle. By default, we use the modified spectral
99 ordering with graph Laplacian \mathbf{L}_{rw} , since we also use \mathbf{L}_{rw} in the spectral clustering. There are no noticeable
100 differences between the normalized \mathbf{L}_{rw} and \mathbf{L}_{sym} in our preliminary studies.

101 **Change of marginal likelihood**

102 We calculate the marginal likelihood for an individual, since offspring are assumed to be independent given
103 the current phased parental genotypes. Let x_t be the latent ancestral origins at locus t , y_t be the observed

104 genotype data, and $y_{(t+1):t+w}$ be the observed genotypic data in the window of loci from $t + 1$ to $t + w$. The
 105 standard forward algorithm recursively calculates the joint probability $P(x_t, y_{1:t})$ forwardly for $t = 1, \dots, M$,
 106 where M is the number of markers. The backward algorithm recursively calculates the conditional probability
 107 $P[y_{(t+1):M}|x_t]$ backwardly for $t = M, \dots, 1$ with initial $P[y_{(M+1):M}|x_M] = 1$. The marginal likelihood is
 108 given by

$$P(y_{1:M}) = \sum_{x_t} P(x_t, y_{1:t}) P[y_{(t+1):M}|x_t]$$

109 since $P[y_{(t+1):M}|x_t, y_{1:t}] = P[y_{(t+1):M}|x_t]$ according to the Markov approximation.

110 The above calculation of $P(y_{1:M})$ is valid for any locus t in a given genetic map, which enables a fast way
 111 to calculate the change $\Delta \log l$ of log marginal likelihood. We update inter-marker distances one by one from
 112 left to right along chromosomes, and update local ordering by sliding a small window along chromosomes.
 113 We first perform the backward algorithm for all offspring. Synchronizing with an update window sliding
 114 along chromosomes, we erase the backwardly calculated $P[y_{(t+1):M}|x_t]$ and meanwhile update the forwardly
 115 calculated $P(x_t, y_{1:t})$ up to the rightmost locus t of the window. For a given update window, we can calculate
 116 the log marginal likelihood for a proposal map and thus $\Delta \log l$ by only re-calculating the forward probabilities
 117 for the loci within the window.

118 **Running setups of map construction packages**

119 ***magicMap***

120 The Mathematica command line used for magicMap is given by

```
121 magicMap[magicsnpfile, model, popdesign, ngroup, options]
```

122 where the `magicsnpfile` specifies the input genotypic data. For simulated data, we set `model` to be
 123 "indepModel" for the F2, "jointModel" for the CP, and "depModel" for the 8-way RIL. For the real data, we set
 124 `model` to be "jointModel" for the Apple CP, and "depModel" for the Arabidopsis 2-way RIL, the Arabidopsis
 125 MAGIC, and the barley multiparental population.

126 The `popdesign` specifies the breeding design information, which is used to compute the process parameter
 127 values of the HMM. `popdesign` is set to be the corresponding simulated pedigree file for all simulated

128 data, the real apple CP data, and the real barley data. For the real *Arabidopsis* 2-way RIL, it is set to be
129 {"Pairing", "Pairing", "Selfing", ..., "Selfing"} where "Selfing" is repeated for
130 8 times. For the AI-RIL, it is set to be {"FullDiallel", "RM1-E-1000", "RM1-E", ..., "RM1-1E",
131 "Selfing", ..., "Selfing"} where "RM1-E" is repeated for 3 times, and "Selfing" is repeated
132 for 6 times. The `nrgroup` specifies the number of linkage groups.

133 There are many options for `magicMap` to specify the details of map construction. We use default option values,
134 except that we set the option `isFounderInbred` \rightarrow `False` for the CP where two parents are outbred,
135 and we set `minLodSegregateBin` \rightarrow `Automatic` for the maize MAGIC and the maize EU-NAM.

136 ***MSTmap***

137 The command line used for `MSTmap` is given by

```
138 MSTmap.exe input.txt output.txt
```

139 Here input file `input.txt` specifies genotypic data and some parameter values, and output file `input.txt`
140 outputs the constructed genetic map. We set `distance_function` to `Haldane`, `missing_threshold` to
141 `1.00`, `estimation_before_clustering` to `no`, `detect_bad_data` to `yes`, and `objective_function`
142 to `ML`.

143 We set `population_type` to `RIL2` for the simulated F2 and to `RIL8` for the real *Arabidopsis* 2-way RIL.
144 For grouping from simulated data, we set `cut_off_p_value` to 10^{-6} for the population size 50 and to 10^{-10}
145 for the other population sizes, and we set `no_map_dist` to 15.0 and `no_map_size` to 2. For ordering from
146 simulated data, we use the grouping results of `magicMap`, and set `cut_off_p_value` to 2, `no_map_dist`
147 to 10^6 , and `no_map_size` to 0. For the real *Arabidopsis* 2-way RIL, we set `cut_off_p_value` to 10^{-12} ,
148 `no_map_dist` to 15.0 and `no_map_size` to 2.

149 ***Lep-MAP3***

150 The command line used for `Lep-MAP3` parental genotype calling is given by

```
151 java -cp ParentCall2 data=geno.post >geno.call
```

152 The command line used for `Lep-MAP3` filtering is given by

```
153 java -cp Filtering2 data=geno.call dataTolerance=0.001 >geno_f.call
```

154 For Lep-MAP3 grouping, first run the following command line

```
155 java -cp SeparateChromosomes2 data=geno_f.call  
156         lodLimit=threshold sizeLimit=5 >geno_f_grouping.txt
```

157 and iteratively run the following command until the grouping does not change

```
158 java -cp JoinSingles2All map=geno_f_grouping.txt  
159         lodLimit=4 >geno_f_grouping_iter.txt
```

160 The command line used for Lep-MAP3 ordering is given by

```
161 java -cp OrderMarkers2 map=geno_f_grouping_iter.txt  
162         data=geno_f.call numMergeIterations=6  
163         useKosambi=0 sexAveraged=1 >geno_f.order
```

164 Here input file `geno.post` specifies genotypic data, output file `geno_f_grouping.txt` saves the group-
165 ing, and output file `geno_f.order` saves the constructed genetic map. Here we set the threshold of
166 `lodLimit` to 6 for simulated data, and 8.5 for the real apple CP data. For marker ordering in the simulated
167 data, we use the grouping obtained from `magicMap`.

168 ***mpMap***

169 The R command lines used for `mpMap` grouping in the simulated 8-way RIL are given by

```
170 dat.rf <- mpestrf(sim.dat)  
171 grouped <- mpgroup(dat.rf, groups=5, clusterBy="combined", method="average")
```

172 Here the object `sim.dat` specifies all genotypic data and pedigree information.

173 The R command lines used for `mpMap` ordering and spacing in the simulated 8-way RIL are given by

```
174 dat.rf <- mpestrf(sim.dat)  
175 grouped <- mpgroup(dat.rf, groups=1, clusterBy="combined", method="average")  
176 ordered2 <- mporder(grouped, 1, type="2")  
177 orderedm1 <- mporder(ordered2, 1, type="m", mapfx="haldane", window=5, repeats=1)  
178 orderedm1d <- computemap(orderedm1, mapfx = "haldane", maxOffset=40)
```


179 Here the object `sim.dat` specifies genotypic data for a given linkage group and pedigree information. The
180 grouping is given by `magicMap`.

181 **Preparation of the real datasets**

182 The marker data for the *Arabidopsis* RIL, the CP, and the barley MAGIC have been filtered by [West *et al.*](#)
183 [\(2006\)](#), [Gardner *et al.*](#) [\(2014\)](#), and [Liller *et al.*](#) [\(2017\)](#), respectively, and they were used directly as the test data.
184 For the *Arabidopsis* MAGIC, the markers with the number of missing founder genotypes being greater than
185 4 and the markers without known physical locations were deleted, there remain 1228 out of 1259 markers.
186 For the tomato MAGIC, 5 out of 1487 markers were deleted because offspring genotypes at those markers
187 are completely missing. For the maize MAGIC ([Dell'Acqua *et al.*](#) [2015](#)), we select 303 out of 529 offspring
188 with eight founders. And we deleted 6700 marker with missing fraction greater than 0.5, 6025 monomorphic
189 markers, and 36 markers with the number of missing founder genotypes being greater than 4, reducing the
190 number of markers from 54234 to 41473. For the marker data of the maize EU-NAM ([Bauer *et al.*](#) [2013](#)), only
191 the markers the are present in the genetic map derived by [Giraud *et al.*](#) [\(2014\)](#) were selected. For the maize
192 US-NAM and the maize EU-NAM, the parental genotypes were imputed and corrected independently for each
193 biparental family, based on single marker analyses; the inconsistent genotypes for the shared parents were then
194 re-set to be missing.

195 To study the effects of the number of markers, we extract four sub-datasets by randomly choosing 2000,
196 5000, 10000, 20000 out of the 41473 markers in the maize MAGIC, and similarly for the 34223 markers in the
197 maize EU-NAM.

198 **Literature Cited**

- 199 Bauer, E., M. Falque, H. Walter, C. Bauland, C. Camisan, L. Campo, N. Meyer, N. Ranc, R. Rincent,
200 W. Schipprack, T. Altmann, P. Flament, A. E. Melchinger, M. Menz, J. Moreno-Gonzalez, M. Ouzunova,
201 P. Revilla, A. Charcosset, O. C. Martin, and C. C. Schon, 2013 Intraspecific variation of recombination rate
202 in maize. *Genome Biology* **14**: R103.
- 203 Brent, R. P., 1973 *Algorithms for Minimization Without Derivatives*. Courier Corporation.
- 204 Dell'Acqua, M., D. M. Gatti, G. Pea, F. Cattonaro, F. Coppens, G. Magris, A. L. Hlaing, H. H. Aung,
205 H. Nelissen, J. Baute, E. Frascaroli, G. A. Churchill, D. Inze, M. Morgante, and M. E. Pe, 2015 Genetic
206 properties of the MAGIC maize population: a new platform for high definition QTL mapping in *Zea mays*.
207 *Genome Biology* **16**: 167–189.
- 208 Ding, C. and X. He, 2004 Linearized cluster assignment via spectral ordering. In *Proceedings of the Twenty-first*
209 *International Conference on Machine Learning*, ICML '04, pp. 30–37, New York, NY, USA, ACM.
- 210 Fiedler, M., 1973 Algebraic connectivity of graphs. *Czechoslovak Mathematical Journal* **23**: 298–305.
- 211 Fiedler, M., 1989 Laplacian of graphs and algebraic connectivity. *Banach Center Publications* **25**: 57–70.
- 212 Gardner, K. M., P. Brown, T. F. Cooke, S. Cann, F. Costa, C. Bustamante, R. Velasco, M. Troglio, and S. Myles,
213 2014 Fast and cost-effective genetic mapping in apple using next-generation sequencing. *G3 (Bethesda)* **4**:
214 1681–1687.
- 215 Giraud, H., C. Lehermeier, E. Bauer, M. Falque, V. Segura, C. Bauland, C. Camisan, L. Campo, N. Meyer,
216 N. Ranc, W. Schipprack, P. Flament, A. E. Melchinger, M. Menz, J. Moreno-Gonzalez, M. Ouzunova,
217 A. Charcosset, C. C. Schon, and L. Moreau, 2014 Linkage disequilibrium with linkage analysis of multiline
218 crosses reveals different multiallelic QTL for hybrid performance in the Flint and Dent heterotic groups of
219 maize. *Genetics* **198**: 1717–1734.
- 220 Liller, C. B., A. Walla, M. P. Boer, P. Hedley, M. Macaulay, S. Effgen, M. von Korff, G. W. van Esse, and
221 M. Koornneef, 2017 Fine mapping of a major QTL for awn length in barley using a multiparent mapping
222 population. *Theoretical and Applied Genetics* **130**: 269–281.
- 223 Shi, J. B. and J. Malik, 2000 Normalized cuts and image segmentation. *IEEE Transactions on Pattern Analysis*
224 *and Machine Intelligence* **22**: 888–905.
- 225 von Luxburg, U., 2007 A tutorial on spectral clustering. *Statistics and Computing* **17**: 395–416.

- 226 West, M. A. L., H. van Leeuwen, A. Kozik, D. J. Kliebenstein, R. W. Doerge, D. A. St Clair, and R. W. Michel-
227 more, 2006 High-density haplotyping with microarray-based expression and single feature polymorphism
228 markers in arabidopsis. *Genome Research* **16**: 787–795.
- 229 Zheng, C., 2015 Modeling X-linked-linked ancestral origins in multiparental populations. *G3 (Bethesda)* **5**:
230 777–801.
- 231 Zheng, C., M. P. Boer, and F. A. van Eeuwijk, 2014 A general modeling framework for genome ancestral
232 origins in multiparental populations. *Genetics* **198**: 87–101.
- 233 Zheng, C., M. P. Boer, and F. A. van Eeuwijk, 2015 Reconstruction of genome ancestry blocks in multiparental
234 populations. *Genetics* **200**: 1073–1087.
- 235 Zheng, C., M. P. Boer, and F. A. van Eeuwijk, 2018a Accurate genotype imputation in multiparental populations
236 from low-coverage sequence. *Genetics* **210**: 71–82.
- 237 Zheng, C., M. P. Boer, and F. A. van Eeuwijk, 2018b Recursive algorithms for modeling genome blocks in a
238 fixed pedigree. *G3 (Bethesda)* **8**: 3231–3245.

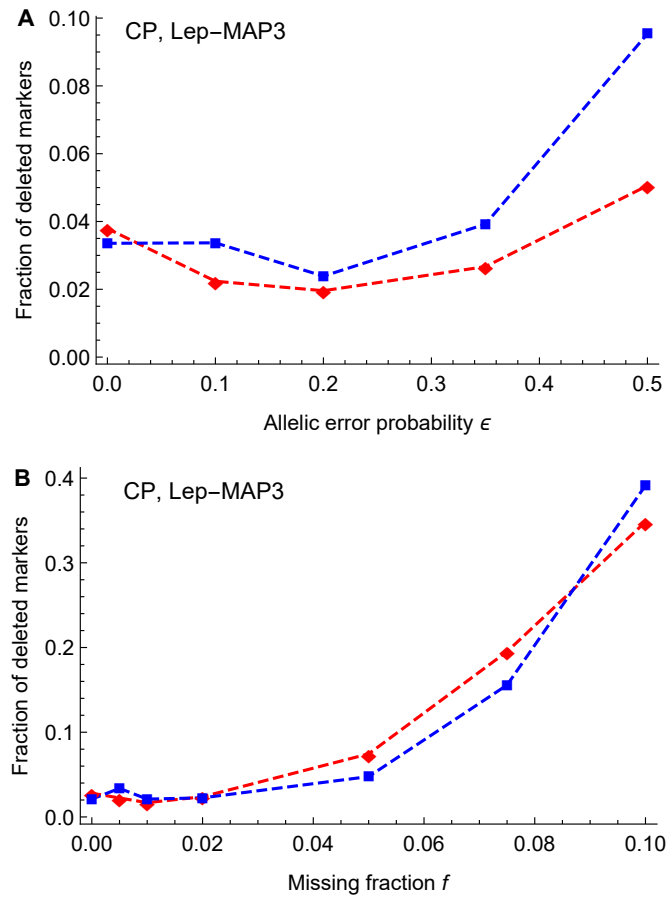


Figure S1 Number of markers deleted during the Lep-MAP3 ordering. The red diamonds (◆) and blue rectangles (■) refer to the CP population sizes of 100 and 200, respectively. (A) Effects of allelic error probability. (B) Effects of missing fraction.

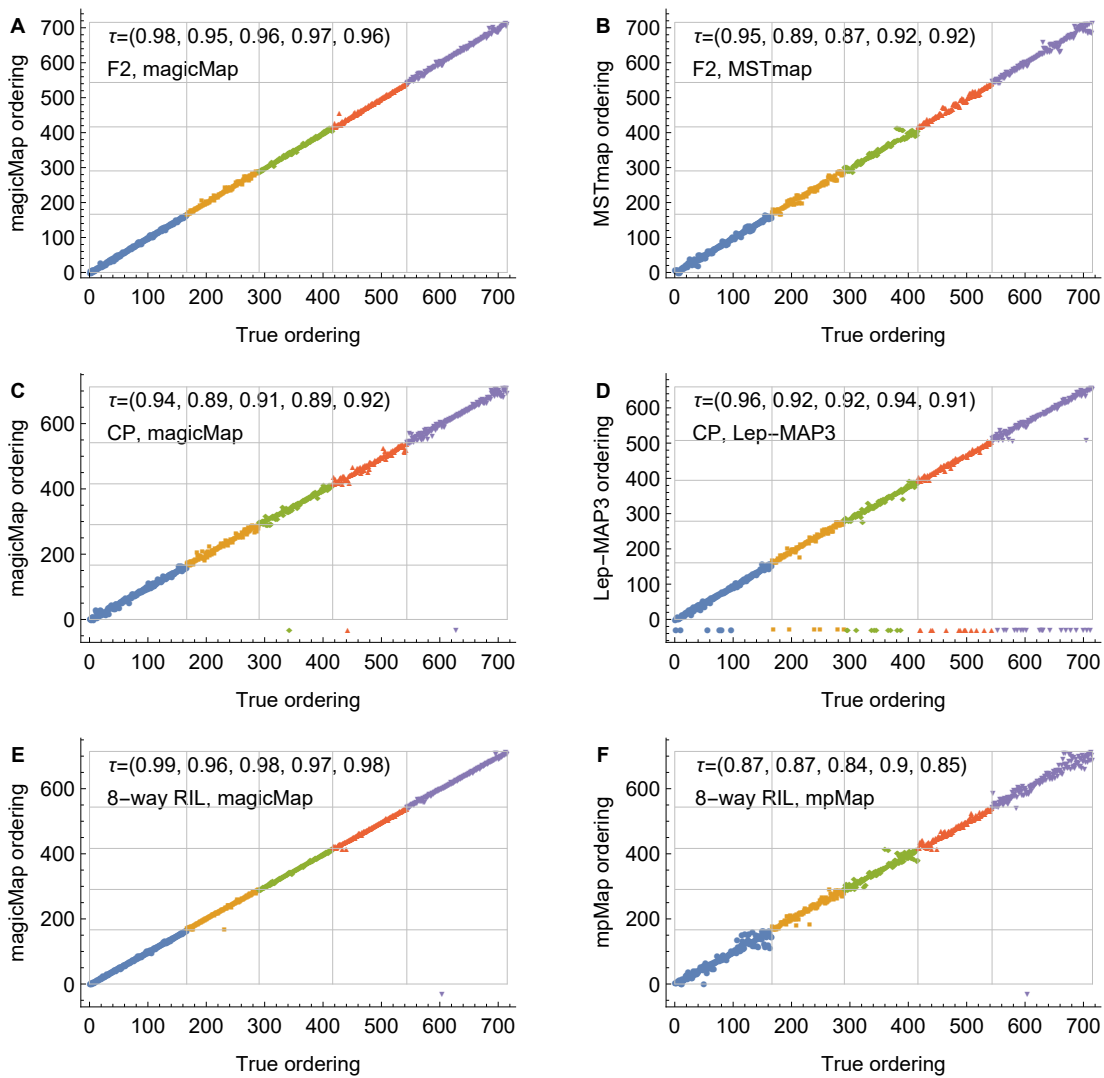


Figure S2 Illustrative comparisons between estimated marker ordering and the true ordering. The left panels refer to magicMap (A, C, and E), and the right panels refer to MSTmap (B), Lep-MAP3(D), and mpMAP (F). The gray grid lines denote the chromosome boundaries, and the dots with negative y-values denote the ungrouped markers. The values of Kendall's tau (τ) for five chromosomes are given for the F2 (A&B), the CP (C&D), and the 8-way RIL (E&F), respectively. The results are obtained from the simulated data with allelic error probability $\epsilon = 0.05$, missing fraction $f = 0.1$, and medium population size 100 for both the F2 and the CP and 400 for the 8-way RIL.

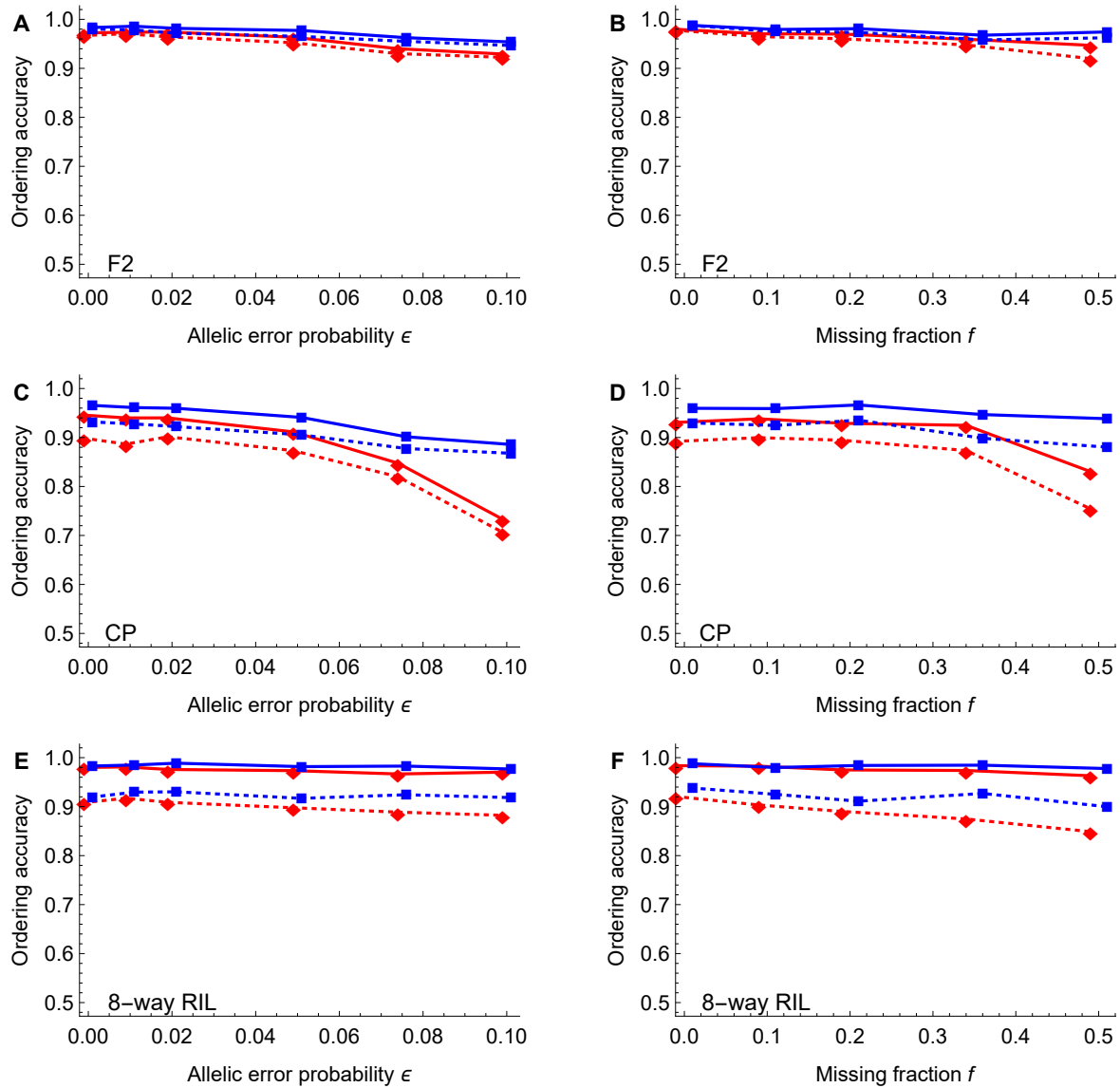


Figure S3 Effect of magicMap ordering refinement. The dotted lines denote the initial spectral orderings, and the solid lines denote the refined ordering. The red diamonds (\blacklozenge) and blue rectangles (\blacksquare) refer to medium and large population sizes, respectively. The population sizes are 100 and 200 for the F2 (A&B) and the CP (C&D), and they are 400 and 800 for the 8-way RIL (E&F).

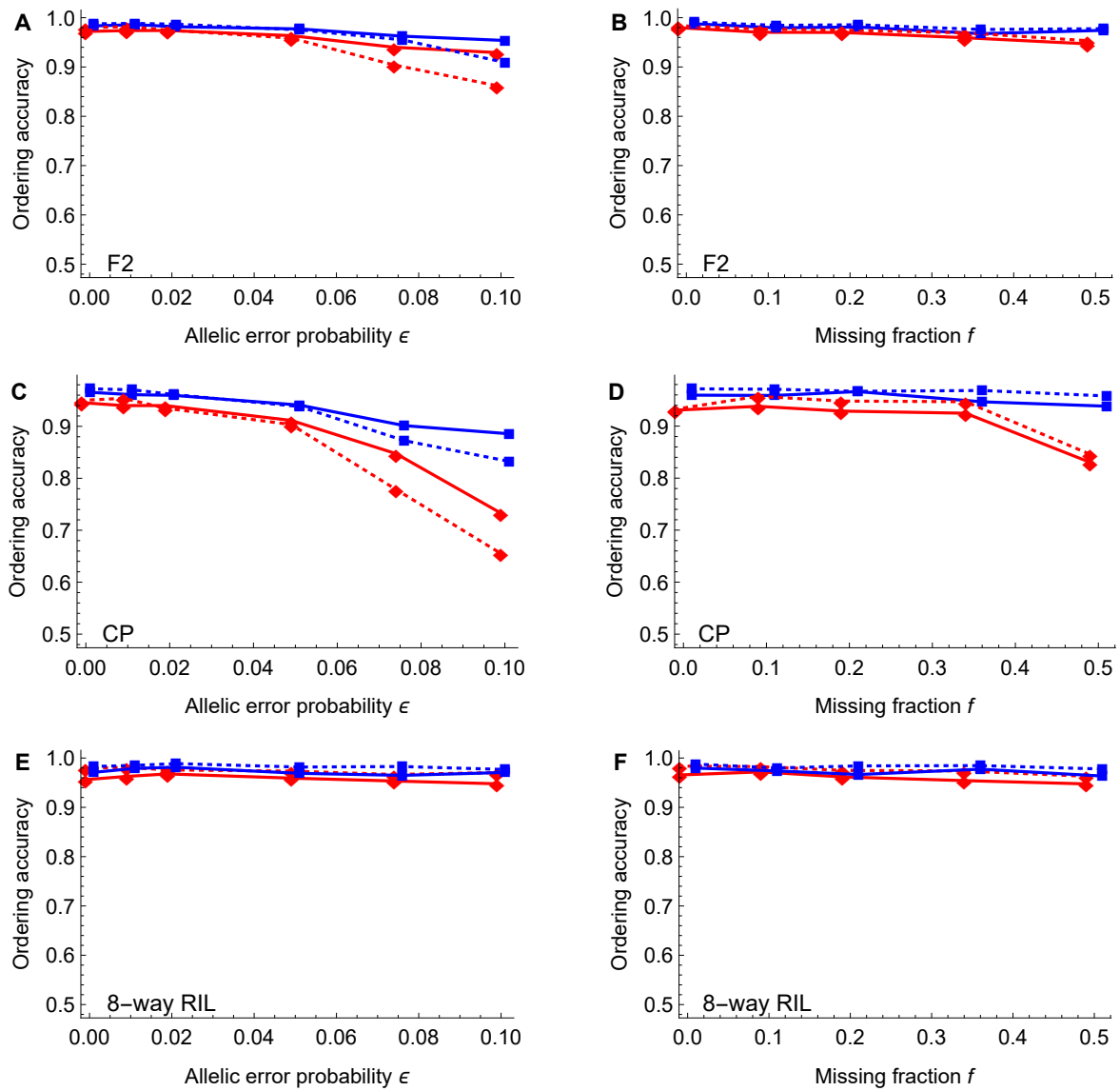


Figure S4 Effect of magicMap error correction on marker ordering. The dotted lines denote the refined orderings without the error correction, and the solid lines denote the orderings with the error correction. The red diamonds (◆) and blue rectangles (■) refer to medium and large population sizes, respectively. The population sizes are 100 and 200 for the F2 (A&B) and the CP (C&D), and they are 400 and 800 for the 8-way RIL (E&F).

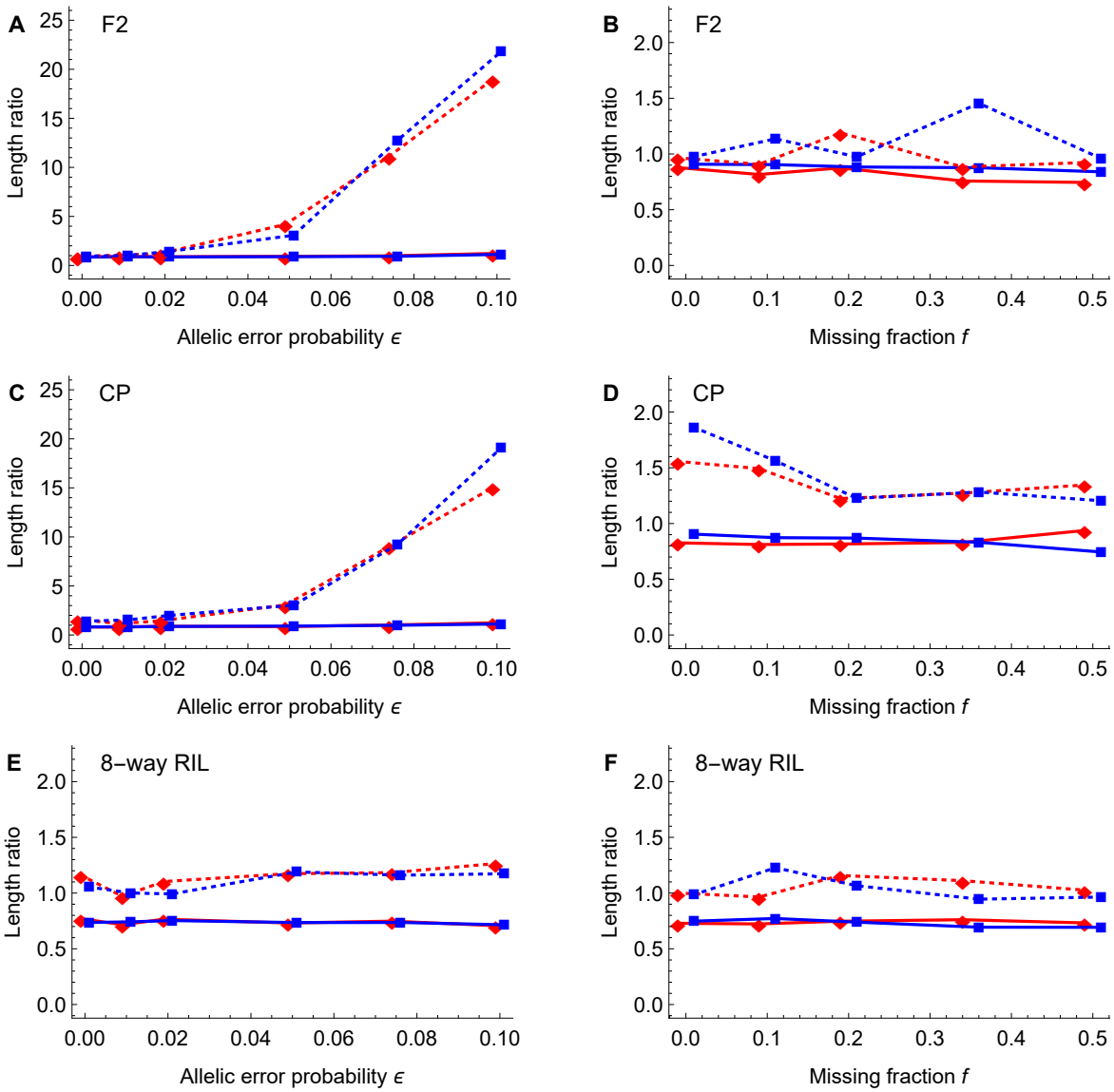


Figure S5 Effect of magicMap error correction on marker spacing. The y-axis denotes the ratio of estimated total chromosome length to true value. The dotted lines denote the refined orderings without the error correction, and the solid lines denote the orderings with the error correction. The red diamonds (♦) and blue rectangles (■) refer to medium and large population sizes, respectively. The population sizes are 100 and 200 for the F2 (A&B) and the CP (C&D), and they are 400 and 800 for the 8-way RIL (E&F).

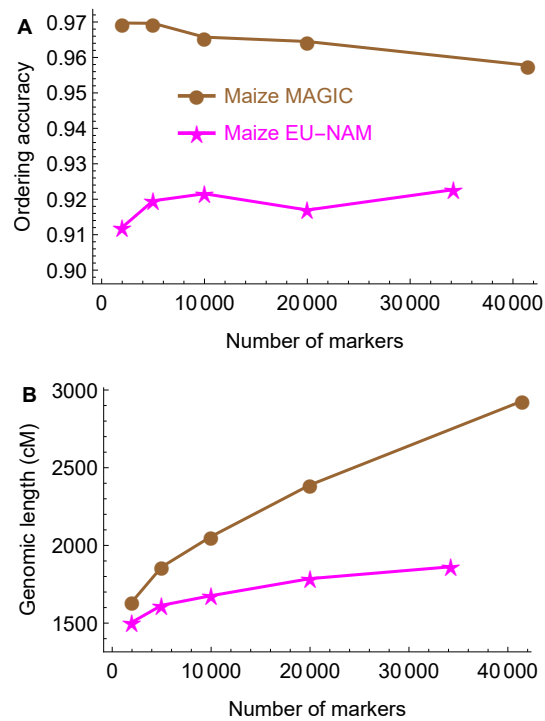


Figure S6 Scaling of magicMap performances with the number of markers in the maize MAGIC and the maize EU-NAM. (A) The ordering accuracy. (B) The genetic map length.

Table S1 List of symbols and their brief descriptions

Symbol	Description
x_t^m	Ancestral origin of the allele on maternally derived chromosome at locus t
x_t^p	Ancestral origin of the allele on paternally derived chromosome at locus t
x_t	Hidden state at locus t . $x_t = (x_t^m, x_t^p)$
d_t	Genetic distance in Morgan between loci t and $t + 1$
$P(x)$	Probability that the implicit random variable takes value x
$P[x_2 x_1, d]$	Transition probability matrix from random variable x_1 to x_2 for a given d value.
"depModel"	Dependent model with $x_t^m = x_t^p$
"indepModel"	Independent model with $P(x_t^m, x_t^p) = P(x_t^m)P(x_t^p)$
"jointModel"	Joint model without assuming a simplified structure of $P(x_t^m, x_t^p)$
I	Identity matrix
Q^m	Rate matrix of Markov process along the maternal chromosome
Q^p	Rate matrix of Markov process along the paternal chromosome
Q	Rate matrix for two homologous chromosomes under "jointModel" $Q = Q^m \otimes I + I \otimes Q^p$ under "indepModel" $Q = (Q^m + Q^p)/2$ for autosomes or female XX under "depModel" $Q = Q^m$ for male X chromosome under "depModel"
$\pi(x)$	Stationary distribution vector as a function of random variable x
R	Expected number of recombination change-points per Morgan
r	Scaled recombination fraction
f	Fraction of missing offspring genotypes
ϵ	Allelic error probability in offspring
ϵ_F	Allelic error probability in founders
y_i^o	Genotype of offspring o at locus $i = 1, 2$
h_i	Parental haplotype at locus $i = 1, 2$
$l(r, h_1, h_2)$	Two-locus likelihood. Probability of all offspring genotypes at loci 1 and 2
G	Test statistic in G-test
C_{save}	LOD score threshold below which the results of two-locus analysis are not saved
$C_{linkage}$	LOD score threshold in linkage analysis
C_{indep}	LOD score threshold in independence tests
S	Similarity matrix $\{s_{ij}\}$
W	Sparse similar matrix $\{w_{ij}\}$ obtained from S
D	Diagonal matrix with i th diagonal element being $\sum_j w_{ij}$
L	Un-normalized graph Laplacian $L = D - W$
L_{sym}	Symmetric normalized graph Laplacian $L_{sym} = I - D^{-1/2}WD^{-1/2}$
L_{rw}	random walk related graph Laplacian $L_{rw} = I - D^{-1}W$
k_{nn}	Number of nearest neighbors
$\Delta \log l$	Change of log likelihood by the proposal map
T	Temperature in simulated annealing
T_0	Initial temperature in simulated annealing
T_c	Freezing temperature in simulated annealing
α	Cooling constant. $T \rightarrow \alpha T$ if $T > T_c$ and $T \rightarrow \alpha^3 T$ if $T \leq T_c$ after each iteration
n_{freeze}	Maximum number of iterations with $T \leq T_c$